Available online at www.sciencedirect.com
SCIENCE DIRECT
Tectonophysics 414 (2006) 145–155
TECTONOPHYSICS
www.elsevier.com/locate/tecto

The lithospheric density structure of the Eastern Alps

Jörg Ebbing [a,*], Carla Braitenberg [b], Hans-Jürgen Götze [c]

[a] Geological Survey of Norway (NGU), 7491 Trondheim, Norway
[b] Department of Earth Sciences, University of Trieste, Via Weiss 1, 34100 Trieste, Italy
[c] Institut für Geowissenschaften, Christian-Albrechts-Universität zu Kiel, Otto-Hahn-Platz 1, 24118 Kiel, Germany

Received 1 September 2004; received in revised form 7 February 2005; accepted 4 October 2005
Available online 5 December 2005

Abstract

The three-dimensional (3D) lithospheric density structure of the Eastern Alps was investigated by integrating results from reflection seismics, receiver function analyses and tomography. The modelling was carried out with respect to the Bouguer gravity and the geoid undulations and emphasis were laid on the investigations of the importance of deep lithospheric features. Although the influence of inhomogeneities at the lithosphere–asthenosphere boundary on the potential field is not neglectable, they are overprinted by the response of the density contrast at the crust–mantle boundary and intra-crustal density anomalies. The uncertainties in the interpretations are in the same order of magnitude as the gravity field generated by the deep lithosphere.

After including the deep lithospheric geometry from the tomographic model it is shown that full isostatic equilibrium is not achieved below the Eastern Alps. However, calculation of the isostatic lithospheric thickness shows two areas of lithospheric thickening along the central axis of the Eastern Alps with a transition zone below the area of the TRANSALP profile. This is in agreement with the tomographic model, which features a change in lithospheric subduction direction.

Keywords: Eastern Alps; Gravity; Isostasy; Lithosphere; Density structure

1. Introduction

In the past five years, new efforts have been made by the international TRANSALP working group and related groups to gain detailed insights into the structure of the lithosphere below the Eastern Alps. The investigation of the gravity field and the density structure is one of the methods adopted to give insights into the 3D structure of the lithosphere. New measurements were carried out in the Italian part of the Eastern Alps to improve the gravity database (Zanolla et al., this volume). Simultaneously, the lithospheric structure of the Eastern Alps was investigated with 3D density modelling (Ebbing et al., 2001; Ebbing, 2004). Density modelling was constrained by the results obtained by the seismic investigations of the TRANSALP Working Group (2001, 2002) and related groups (Kummerow, 2002; Kummerow et al., 2004). Regarding the upper mantle, different authors have proposed a lithospheric root below the Eastern Alps (Suhadolc et al., 1990; Babuŝka et al., 1990; Lippitsch et al., 2003; Panza et al., 2003), which should have also an influence on the gravity field. Unfortunately, these latter models are not completely consistent with each other and there is no general agreement about the geometry of the base of the lithosphere. As the geometry of the base lithosphere can cause a significant response in the gravity signal and the geoid (Lillie et al., 1994), the lithospheric models

* Corresponding author. Tel.: +47 73 90 4451; fax: +47 73 90 4494.
E-mail address: Joerg.Ebbing@ngu.no (J. Ebbing).

0040-1951/$ - see front matter © 2005 Elsevier B.V. All rights reserved.
doi:10.1016/j.tecto.2005.10.015

must be combined with crustal models to give a complete picture of the collision zone between the European and Adriatic plate.

In this paper we provide a short overview of recent studies dealing with the density structure and the isostatic state of the Eastern Alps, focussing especially upon the studies in the framework of the TRANSALP project. In addition, a complete lithospheric 3D density model is presented, including a discussion of the lithospheric root. We will discuss the difficulties and pitfalls of a complete lithospheric model concerning the resolution of deep-seated domains. The implications of our model for the isostatic state of the Eastern Alps are investigated by calculating loads and related vertical stresses at different lithospheric depths and by calculating an isostatically balanced lithosphere–asthenosphere boundary.

2. Crustal structure of the Eastern Alps

The results of the seismic TRANSALP project (TRANSALP Working Group, 2001, 2002) initiated the construction of a new 3D density model of the Eastern Alps (Figs. 1 and 2). The information from e.g. reflection seismic data, receiver function analysis, seismic velocity models and geological models allowed constructing a well-constrained 3D crustal model. However, uncertainties in the geometry of the crust–mantle boundary below the Adriatic plate exist due to certain discrepancies between the constraining information (Ebbing et al., 2001; Ebbing, 2004).

General agreement exists about the density structure of the upper 10 km of the crust. The uppermost part of the crust can be linked directly to geological formations visible at the surface, and this part accounts for up to one third of the total Bouguer gravity field of the Eastern Alps (Cassinis et al., 1997; Ebbing et al., 2001). However, the situation in the middle and lower crustal structure is less clear. In the middle crust the consequences of different tectonic concepts on the 3D density structure are minor. However, the depth to the crust–mantle boundary below the Adriatic plate is more important (Ebbing, 2004). Different models of the 3D density structure have been proposed, with a depth of the crust–mantle boundary between 30 and 40 km (Cassinis et al., 1997; Ebbing et al., 2001; Ebbing, 2004), according to the constraining information adopted (e.g. Giese and Buness, 1992; Scarascia and Cassinis, 1997; TRANSALP Working Group, 2002; Kummerow, 2002).

In this paper we study the effect of the possible presence of a lithospheric root on the gravity modelling,

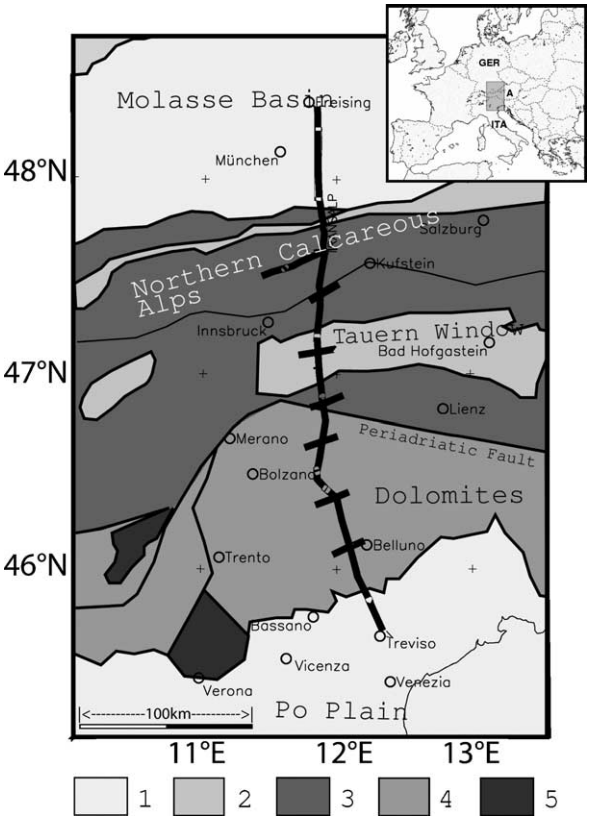

Fig. 1. Geology of the Eastern Alps. The large map is a simplified tectonic map of the study area. The thick black line shows the location of the TRANSALP seismic profile. Alpine units: 1 = Molasse basins, 2 = Penninic units, 3 = Austroalpine and Helvetic units, 4 = Southern Alps, 5 = Plutonic intrusions. The small inset map shows the location of the study area (grey rectangle). GER, A and ITA denote Germany, Austria and Italy, respectively.

adding the geometry of the lithosphere after Lippitsch et al. (2003) to the model presented in Ebbing (2004) (Fig. 2).

The 3D density model of Ebbing (2004) is based on the results of the TRANSALP reflection seismic and receiver function analysis and on geological interpretation of those data (Kummerow, 2002; TRANSALP Working Group, 2002). The results of the reflection seismic experiments constrain the base of the crust along most of the transect in Fig. 2. In the central part, the crustal root area, only the receiver function results provide information about the geometry of the crust–mantle boundary. The interpretation of crustal thickness in the Adriatic plate in the present paper is slightly different to the models in Ebbing (2004). In the transition between European and Adriatic plate the crustal thickness is about 40 km. Consequently the density of the lower crust below the Southern Alps had to be increased to 3050−3100 kg/m^3 to give a

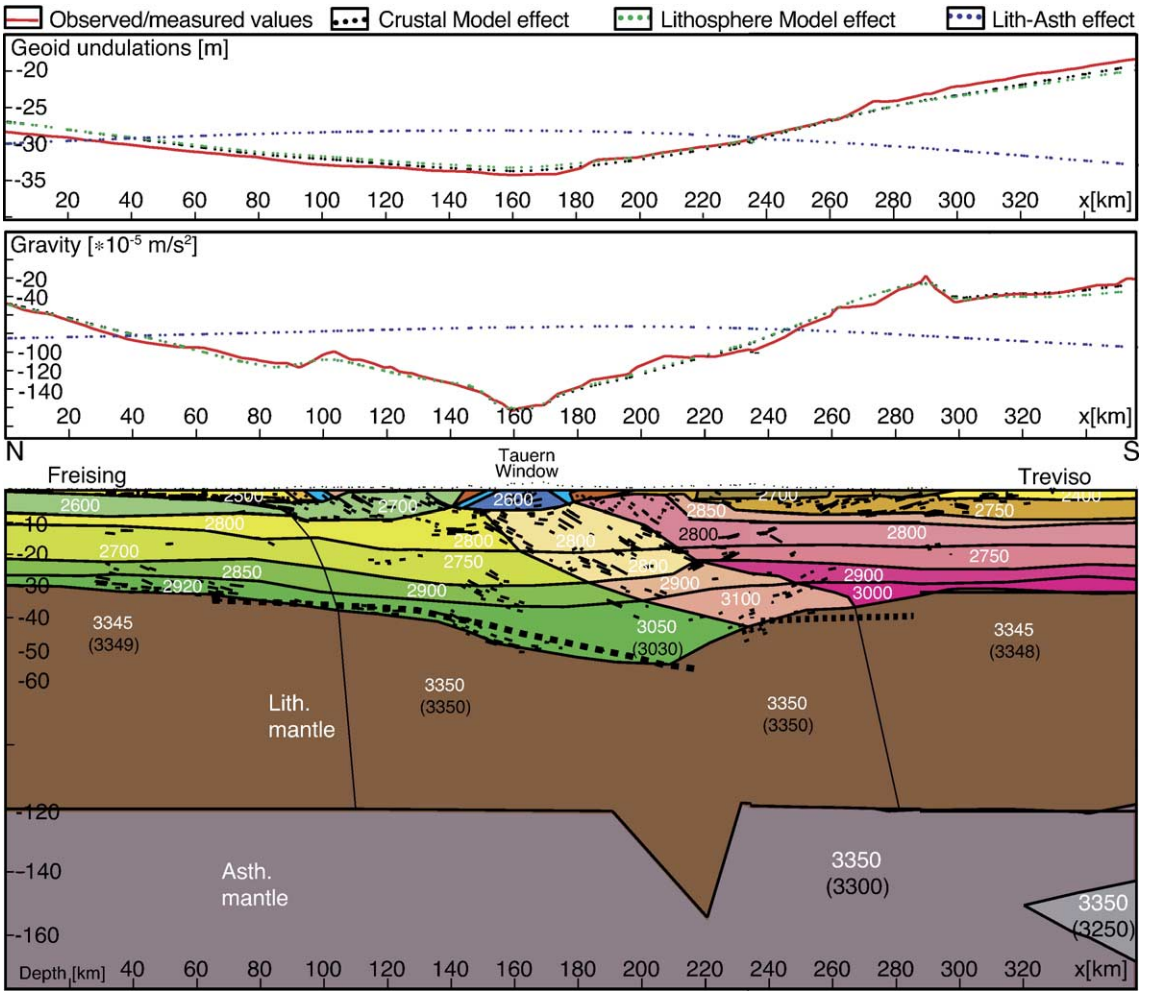

Fig. 2. Cross-section through the 3D density model. The cross-section is located along the TRANSALP seismic profile line (see Fig. 1 for location). The lower part shows the density structure of the lithosphere and upper asthenosphere. The model shows the crustal model (Ebbing, 2004) and the deep lithospheric geometry following the tomographic model by Lippitsch et al. (2003). Greenish colours indicate European, reddish colours Adriatic and brownish colours mantle domains. Colours of surface structures relate to the geological map of Berthelsen et al. (1992). White numbers indicate density values in kilogram per cubic meter for the crustal model with a small contribution from the deep lithosphere. Alternative densities (black) for the mantle are used to demonstrate the effect of combined crustal geometry and lithosphere–asthenosphere boundary on the gravity field and the geoid undulations. Central and upper part show gravity field and geoid undulations, respectively. Shown are the observed field (Bouguer anomaly/topographic reduced geoid), gravity effect of crustal and lithospheric, and the gravity response of the lithosphere–asthenosphere boundary with a constant density contrast of -50 kg/m^3 and additional -50 kg/m^3 for Po Plain anomaly. The black lines are line-drawings of Vibroseis experiments (TRANSALP Working Group, 2002) and the thick dashed line indicates crust–mantle boundary from receiver function analysis (Kummerow, 2002).

reasonable fit between the modelled and observed potential fields. However, a density value larger than 3000 kg/m^3 is not likely to represent normal continental lower crust. The modified model shows the Adriatic crustal thickness thinning to about 30 km within the Adriatic plate, featuring only a thickened crust in the transitional area. Here, crustal doubling and connected compression forces due to the collision process can explain the high-densities, which is in agreement with regional isostatic studies (Ebbing, 2004).

3. Lithospheric structure of the Eastern Alps

Evaluation of lithosphere–asthenosphere models published by different authors (Babuŝka et al., 1990; Suhadolc et al., 1990) showed that these models are not of sufficient resolution in the study area to be used for gravity modelling purposes (see also the detailed discussion of the quality of these models given by Kissling, 1993). Recent tomographic results from Lippitsch (2002) and Lippitsch et al. (2003) show clearly the

subduction of the Adriatic lithosphere below the European lithosphere.

Modelling of the complete lithosphere is difficult due to the uncertainties underlying the models of the lithosphere–asthenosphere boundary. In previous studies (Braitenberg et al., 1997; Ebbing et al., 2001) we adopted the lithosphere–asthenosphere boundary by Suhadolc et al. (1990). While the influence on the Bouguer gravity was not prominent, the influence on the geoidal signal was clear. It produced a north–south oriented residual.

The same observations can be made for the lithospheric model by Babuška et al. (1990), which shows a different geometry for the base of the lithosphere. Here, the uncertainties in the geometry of the lithosphere–asthenosphere system are even higher than in the model of Suhadolc et al. (1990) due to the method of analysis (Kissling, 1993).

Within the framework of the TRANSALP project new tomographic data were collected and interpreted, which ought to provide a more reliable picture of the deep-seated domains (Kummerow et al., 2004; Lippitsch et al., 2003; Panza et al., 2003). However, the results of the studies are ambiguous, but all show lithospheric anomalies below the Eastern Alps.

We combined the tomographic model of Lippitsch et al. (2003) with the 3D density model TRANSALP of Ebbing (2004), with the modification discussed above. The model of Lippitsch et al. (2003) was suitable for this purpose as it provides the 3D velocity variations in this area. According to their model, the European lithosphere should be subducting below the Adriatic plate in the Western Alps and western Eastern Alps, while in the easternmost Eastern Alps the Adriatic lithosphere should be subducting below the European lithosphere. The central Eastern Alps lie between the two different subducting plates and overly the area where the subduction direction is changing.

Our 3D lithospheric density model is extended to 400 km depth to cover all anomalies related to the lithosphere. The lithospheric roots were modelled with a higher density compared to the surrounding normal asthenospheric material, with values that are allowed to vary between 20 and 100 kg/m^3. These values define an upper and lower margin of expected lithosphere–asthenosphere density contrasts. The smaller contrast is in agreement with investigations of the lithosphere–asthenosphere boundary below the Eastern Alps–Western Carpathian–Pannonian Basin region (Lillie et al., 1994), as well as with global reference models (e.g. PREM: Dziewonski and Anderson, 1981). The higher density contrast is chosen as an upper limit to demonstrate the maximum effects of deep-seated inhomogeneities. The tomographic model also shows high velocity contrasts, which support the calculation with this value.

Fig. 2 shows a cross-section through the 3D density model with the lithosphere–asthenosphere boundary adapted from Lippitsch et al. (2003). The cross-section is located along the TRANSALP profile in the central Eastern Alps. This is the beginning of the transition between southward subduction (west) and northward subduction (east), but where the lithospheric root is still oriented southward. Below the Po Plain a second feature is visible, the Po Plain anomaly, an area of lower P-wave velocities in the mantle. The influence of the lithosphere–asthenosphere geometry on the gravity field and geoid undulations is shown in Figs. 2–4.

In the first calculation the density contrast between the lithosphere and the asthenosphere was 20 kg/m^3 in general and 40 kg/m^3 for the Po Plain anomaly. These values result in a maximum gravity anomaly of $12.5*10^{-5}$ m/s^2 (Fig. 3c) and a deflection of the geoid of 3 m (Fig. 4c). These values are not high enough to be clearly identified within in a whole lithospheric model and are within the error range of the Bouguer gravity calculation (Zanolla et al., this volume). In the second approach the density contrast between the lithosphere and the asthenosphere was chosen to be 100 and 150 kg/m^3 for the area of the Po Plain anomaly. The high-density contrasts lead to higher anomalies, yielding a maximum amplitude of $40*10^{-5}$ m/s^2 and the related deflection of the geoid in the order of 6 m. Compared to the total amplitude of the Bouguer gravity of around $250*10^{-5}$ m/s^2 and the geoid undulations of 25 m, these values are not neglectable. However, their influence is limited to a very long wavelength of over 300 km. To resolve the influence of the lithospheric anomalies the complete lithospheric model has to be regarded.

The 3D model features the geometry of the model by Lippitsch et al. (2003) and the modified crustal model TRANSALP (Ebbing, 2004). The modelling of the complete lithosphere shows that the deep lithosphere cannot be adequately resolved. In Fig. 2 the response of (1) the "normal" crustal model, (2) the combined lithospheric model and (3) the pure lithosphere–asthenosphere boundary is shown. The adjustments necessary to reproduce the anomalies due to the new deep lithospheric geometry can be made with minor changes of the upper lithospheric mantle densities. These changes lie in the range of 50−100 kg/

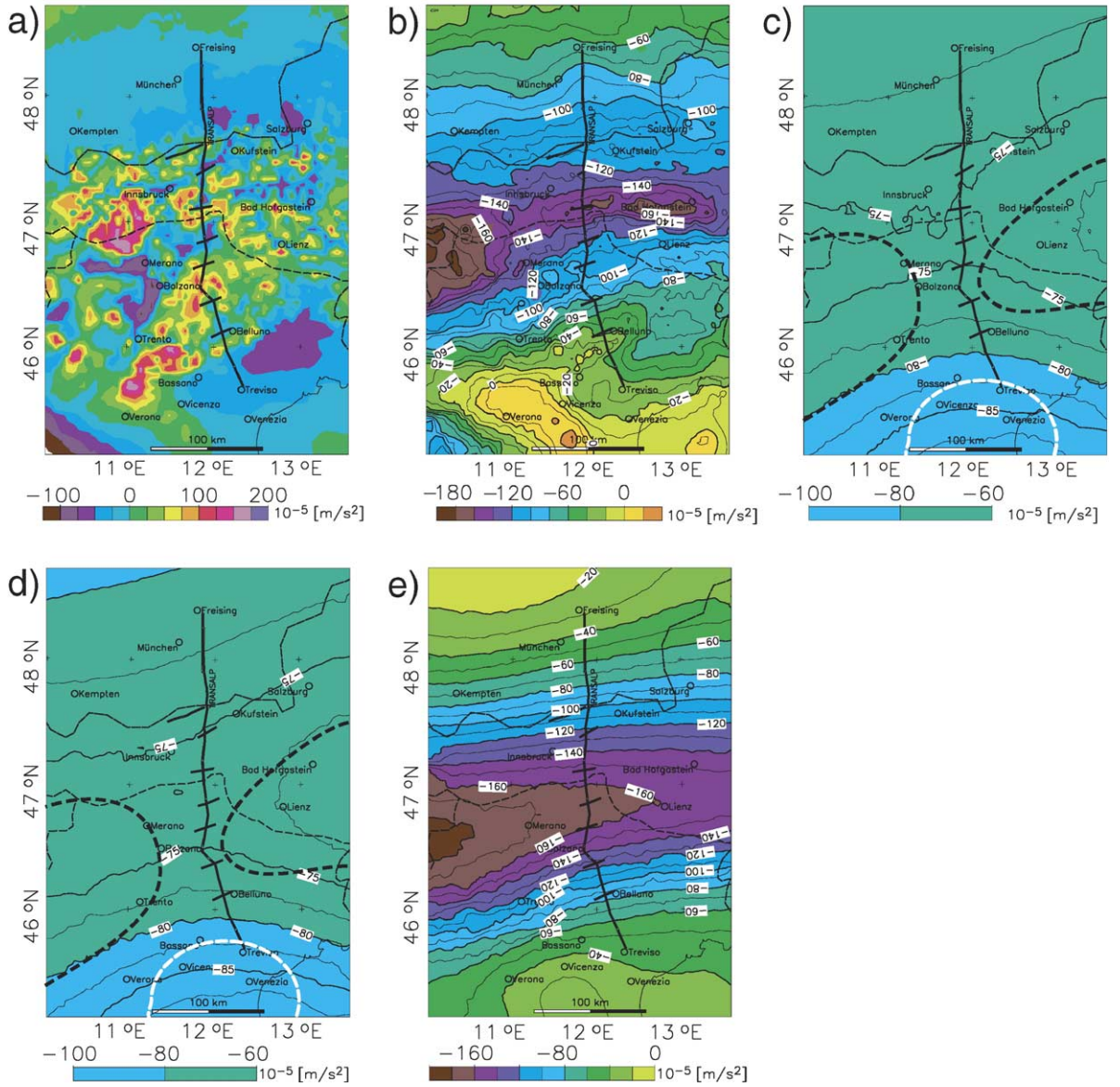

Fig. 3. Observed and calculated gravity fields. a) Free-Air anomaly; b) Bouguer anomaly; c) gravity effect of lithosphere–asthenosphere density contrast (−20 kg/m^3) and Po Plain anomaly (−20 kg/m^3); d) gravity effect of lithosphere–asthenosphere density contrast (−100 kg/m^3) and Po Plain anomaly (−50 kg/m^3); e) gravity effect of crust–mantle density contrast (350 kg/m^3). The bold dotted lines in (c) and (d) indicate the lithospheric root (black) and the Po plain anomaly (white) after Lippitsch et al. (2003).

m^3. Alternatively the densities within the crust can be changed to adjust the model to the measured anomalies, but again changes of density values in the order of 50 kg/m^3 lead to satisfying results. But a value of this order is within the error of the density estimation by velocity–density conversions (Sobolev and Babeyko, 1994).

To demonstrate the difficulties in clearly identifying the influence of the deep lithospheric density structure on the gravity field, the gravity effect and geoid deflection related to the crust–mantle boundary are shown in Figs. 3(e) and 4(e). The density contrast was chosen to be −350 kg/m^3, a value that is normally applied to the crust–mantle boundary (Wagini et al., 1988; Klingele and Kissling, 1982; Götze et al., 1991; Braitenberg et al., 1997, 2002; Ebbing et al., 2001). The gravity and geoid effects are in the same order as the observed fields and clearly overprinting the deep-sourced anomalies. However, the comparison between this Moho-related field and the observed field

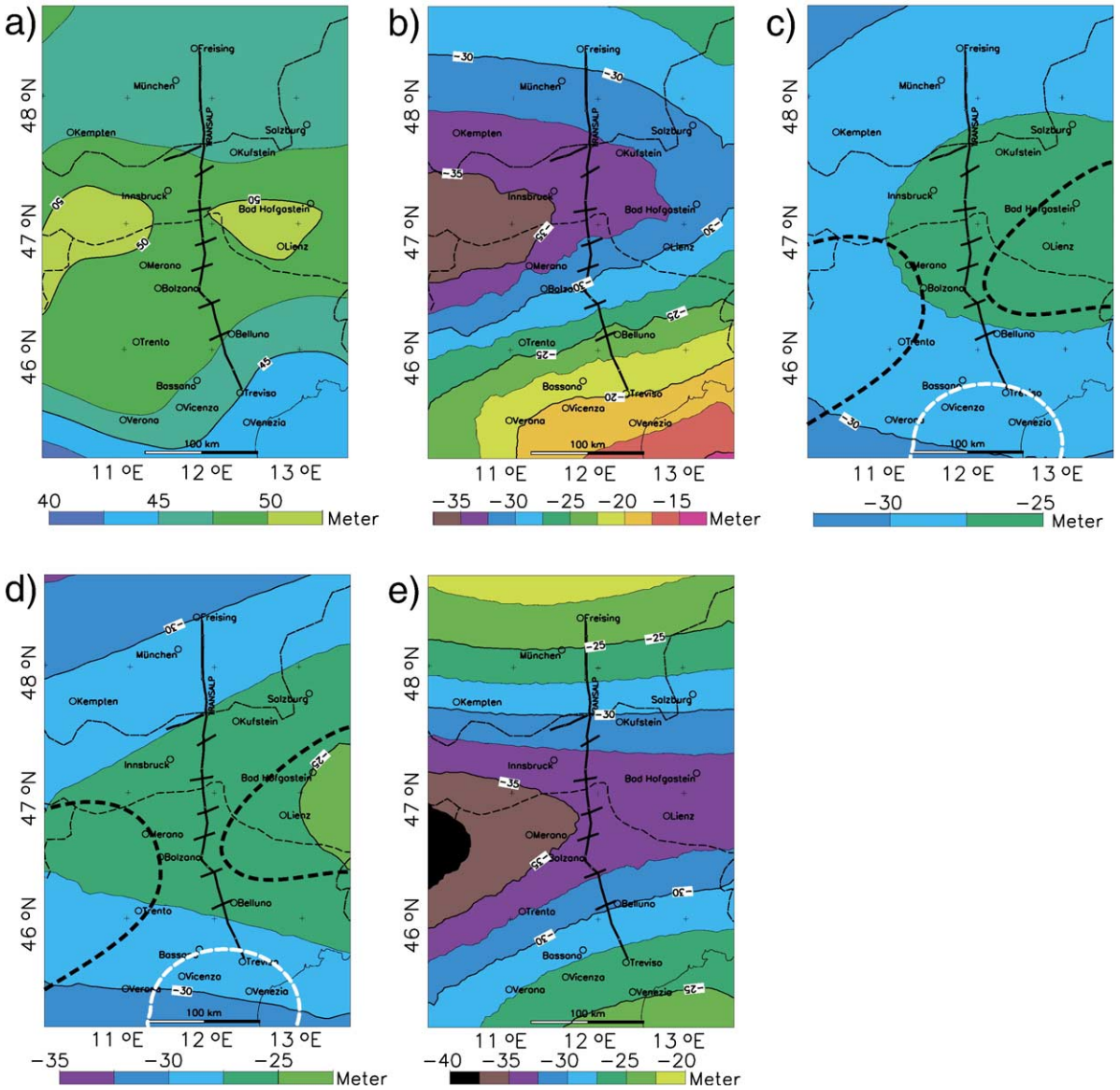

Fig. 4. Observed and calculated geoid undulations. a) Observed geoid (after Lelgemann and Kuckuck, 1992); b) topographic reduced geoid undulations; c) geoid effect of lithosphere–asthenosphere density contrast (−20 kg/m^3) and Po Plain anomaly (−20 kg/m^3); d) geoid effect of lithosphere–asthenosphere density contrast (−100 kg/m^3) and Po Plain anomaly (−50 kg/m^3); e) geoid effect of crust–mantle density contrast (350 kg/m^3). The bold dotted lines in (c) and (d) indicate the lithospheric root (black) and the Po plain anomaly (white) after Lippitsch et al. (2003).

shows the need to consider also the crustal and mantle density domains.

4. Isostasy and loading

The Eastern Alps deviate from the condition of an Airy type local isostatic equilibrium with pure topographic load, as is seen from the simple observation that the Bouguer-minimum falls south of the greatest elevation of topography and that the maximum observed crustal thickness is greater than expected from topographic loading (e.g. Wagini et al., 1988; Götze et al., 1991). The local isostatic residuals correlate well with geological structures at the surface and measured uplift rates (Ebbing, 2004; Zanolla et al., this volume). It is therefore necessary to consider buried crustal loads that derive from density inhomogeneities within the lithosphere (Banks et al., 2001). The gravity modelling described in the previous paragraphs has produced a full 3D density model from

which the topographic and inner crustal loads can be estimated.

We use the lithospheric 3D density model to calculate crustal and topographic loads at different lithospheric depths. These are of interest when considering the lithospheric stresses, as the deviatoric tension or compression within plates caused by lateral thickness and/or density variations can be as important as plate-boundary stresses (Ranalli, 1995). The vertical loading stress at a certain depth is calculated from the vertical integral of the density multiplied by the gravity value. As a first approximation gravity is assumed constant at 9.81 m/s^2. In order to compare the loading stress with the vertical stress expected for a reference lithosphere, we subtract the corresponding reference value obtained from integrating the density column of the reference model. The reference model is divided into 4 layers: the upper crust (0−10 km: 2670 kg/m^3), the lower crust (10−32 km: 2850 kg/m^3), the upper mantle (32−120 km: 3350 kg/m^3), and the asthenosphere (120−300 km: 3300 kg/m^3). For the calculation of the loads and the potential fields, we applied constant densities to the lithospheric and asthenospheric mantle, with a constant density contrast of 50 kg/m^3 (100 kg/m^3 for Po Plain anomaly) between lithosphere and asthenosphere. The reference load and corresponding vertical stress at different depths are given in Table 1.

In Fig. 5 the residual loading stress for depths of 10, 30, 60, 90, 150, and 300 km is shown. At a depth of 10 and 30 km the residual stress is positive below the alpine crest and near zero or negative below the molasse basin in the north and south, due to an excess and deficit of mass, respectively. Below the Moho (from 60 km and below), the relative variation of the residual stress does not vary significantly, maintaining a picture of negative values below the alpine crest and more positive values to the north and south. The small changes are due to small density variations in the upper lithospheric mantle correlating with the Adriatic and European plate and the transitional area (see Fig. 2).

Table 1
The reference load and vertical stress at different depths obtained for the reference model

Depth in km	Load in 10^7 kg/m^2	Vertical stress in MPa
10	3	255
30	8	814
60	18	1795
90	28	2776
150	483	47,333
300	978	95,892

But a relative stress-maximum is found in correspondence to the Vicenza–Verona gravity high.

The influence of the lithosphere root on the stress variation at depth does not significantly alter this picture, although it somewhat reduces the calculated residual stress along the alpine crest for depths greater than 300 km. Our results confirm that even at the depth of 300 km the isostatic local type equilibrium is not achieved, as otherwise the residual stress should be uniformly equal to zero from a certain depth on.

If we assume that the Eastern Alps are in local isostatic equilibrium we can calculate an isostatic lithospheric thickness, assuming constant pressure below the lithospheric root. We adopt the crustal structure of the 3D model and use this to calculate the geometry of the base of the lithosphere needed to achieve isostatic equilibrium. The isostatic lithosphere thickness was calculated with a density contrast at the base of the lithosphere of 50 kg/m^3. The resulting lithospheric thickness (Fig. 6) shows a lithospheric root along the central topographic axis of the Eastern Alps. This lithospheric root is not uniform, but divided into two domains to the west (maximum thickness of 210 km) and east (maximum thickness of 160 km) of the TRANSALP profile. These two lithospheric roots are similar to the tomographic lithospheric model of Lippitsch et al. (2003).

Below the Southern Alps and the Po Plain the isostatic lithosphere thins to only 70 km. This area corresponds to the Vicenza–Verona gravity high, where also the largest loading stresses exist. The Po Plain tomographic anomaly is not expressed in the isostatic lithospheric thickness. As a sub-lithospheric anomaly with lower velocities and densities, it should lead to a thinning of the lithospheric thickness, which we cannot observe. Probably the density contrast of the Po Plain anomaly body and its associated loading are only small. In general, the differences between the isostatic and the tomographic lithosphere thickness are in the order of 10% (~20 km). This is a rather good correlation, as the calculation of the isostatic lithosphere cannot reflect the more complicated subduction geometry expressed in the tomographic model. We have also investigated the extent to which the crustal structure complies to the regional isostatic compensation model of a flexed plate. The flexure model allows laterally variable flexural rigidity and considers both the topographic and inner crustal loading. The inversion of the flexural rigidity was obtained with high spatial resolution by application of the convolution method (Braitenberg et al., 2002). As explained above, the upper crustal structure down to a depth

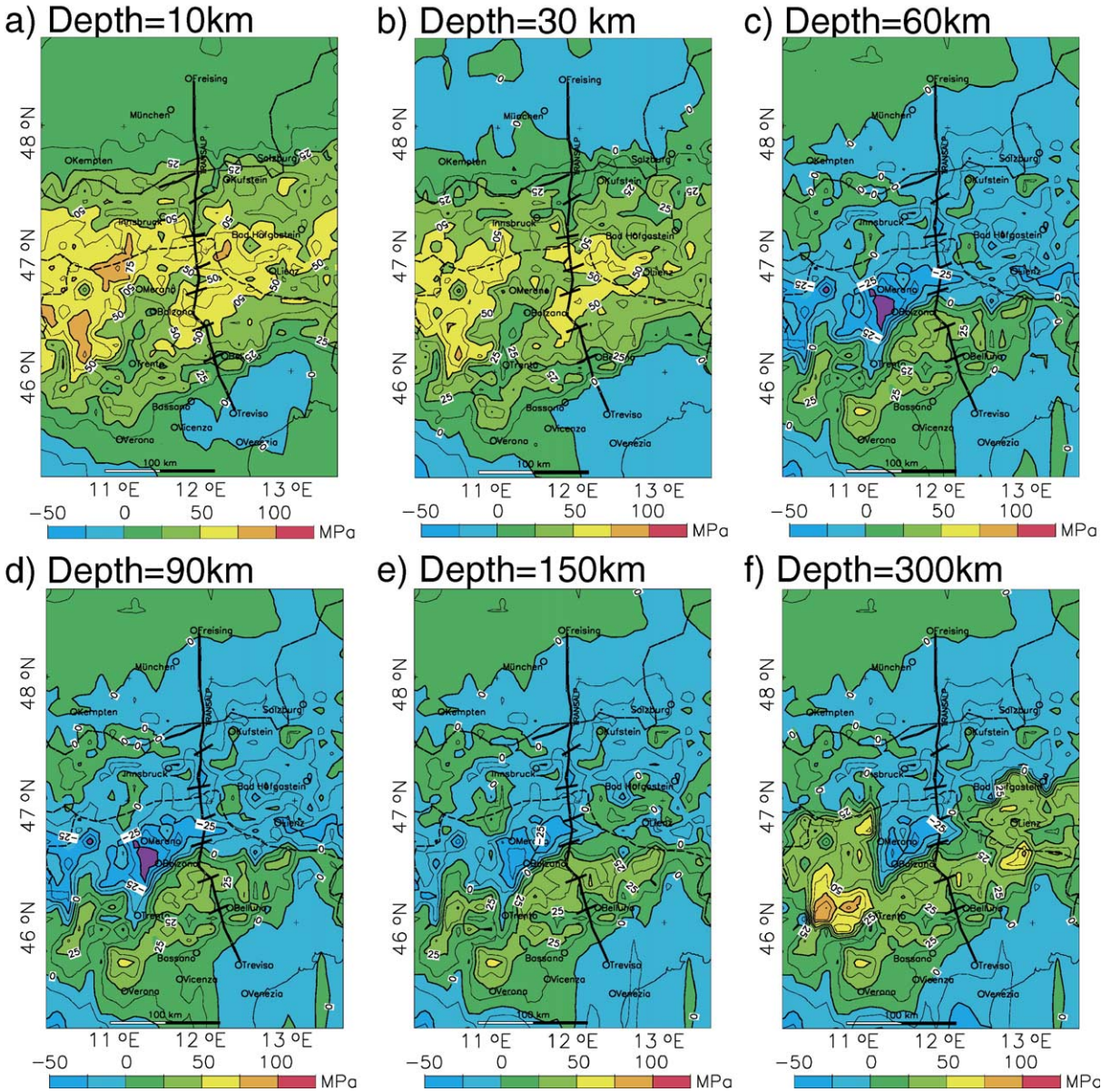

Fig. 5. Vertical loading stress (MPa) below the Eastern Alps for a variety of depths. The values are calculated relative to a "normal" reference crust.

of about 10 km is defined, but greater uncertainties exist regarding the lower crust. Particularly with regard to the thickness of the Adriatic crust, older models have set it to about 30 km (e.g. Giese and Buness, 1992; Cassinis et al., 1997), whereas the recent results in the frame of the TRANSALP working group have set it to about 40 km.

As explained in detail by Braitenberg et al. (2002) and Ebbing (2004), different models were considered in the investigation of the isostatic state adopting the thin plate flexure model. Here we summarize the main results and refer to the above-cited papers for all details. The upper crustal loads are of the same order of magnitude as the topographic loads and cannot be neglected. The central axis of the orogen is characterized by low values of flexural rigidity. The rigidity increases to the north towards the molasse basin and to the south towards the Po basin. Over the greater part of the studied area, the predicted crustal thickness from the flexure model is in good agreement with the model thickness within 2–3 km discrepancy. Exceptions are given by the Vicenza/Verona gravity high and also along the axis where the model Moho reaches its deepest values (SE and NW of Bolzano). The regional

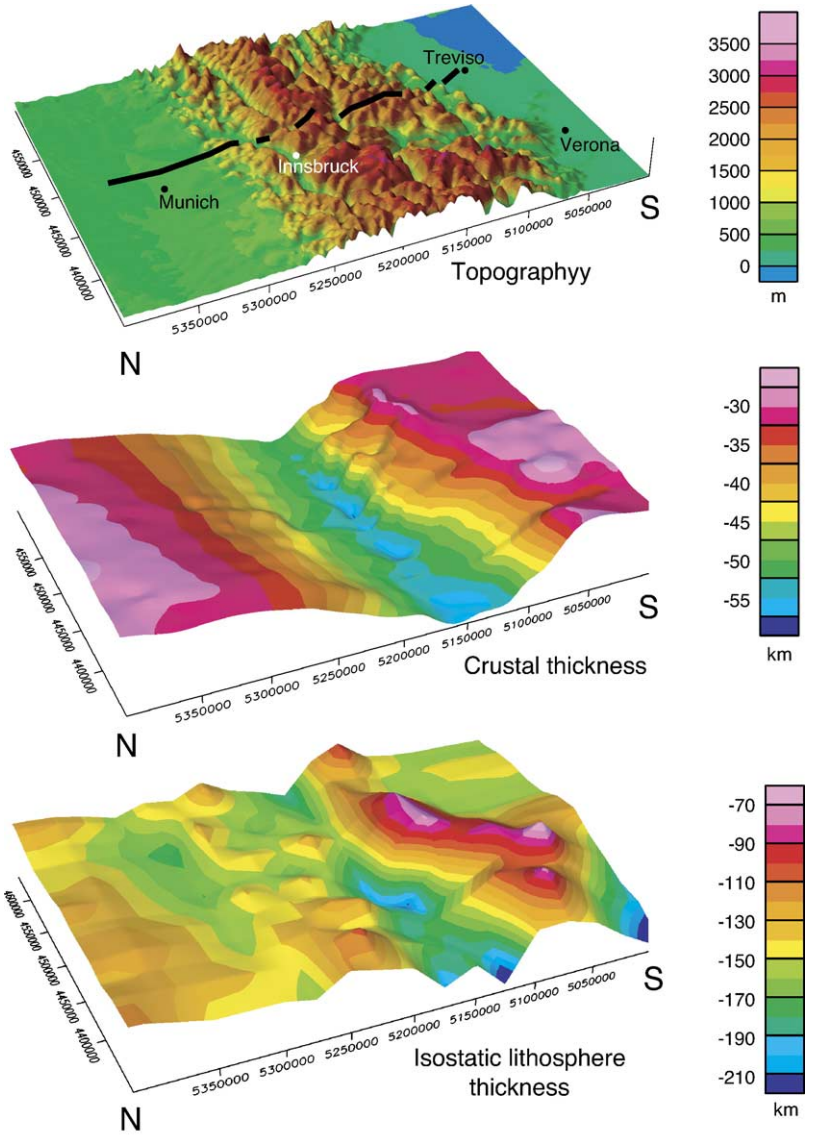

Fig. 6. Topography, crustal thickness and isostatic lithosphere thickness in a perspective view from the north-west. Topography (vertical exaggeration 10×) after GTOPO30 data set (US Geological Survey, 2000) and crustal thickness (vertical exaggeration 2×) from the 3D model. The isostatic lithosphere thickness (vertical exaggeration 1/2×) was calculated by assuming isostatic equilibrium at the base of the lithosphere and loading by the crustal model TRANSALP (Ebbing, 2004). The density contrast at the base of the lithosphere is 50 kg/m^3.

isostatic flexure model therefore also supports the lithosphere thickness variations inferred from the local isostatic equilibrium. A 40 km thick crust of the Adriatic plate does not fit the flexural isostatic model, as it results in too large values for the flexural rigidity of the lithosphere. Crustal doubling could be the reason for the thick crust, which would lead to a surplus of masses to the flexural calculations, which should not be considered in a simple thin plate model. Consequently, a model with 30 km crustal thickness is in better agreement with a regional isostatic model.

5. Discussion and conclusion

We have presented a complete lithospheric model of the Eastern Alps and have shown that even with the combined efforts of seismic and gravity investigations to resolve the lithospheric structure of the Eastern Alps, some unknowns remain. One problem is the reliability of the seismic results supporting the models, especially for deep-seated, sub-crustal inhomogeneities. Another problem is the reliability of the processing of the gravity data. Recent discussion of the geophysical indirect

effect shows that use of ellipsoidal instead of orthometric heights can lead to contributions of a similar magnitude and wavelength as discussed in our example (e.g. Hackney and Featherstone, 2003).

Even assuming that our database is unaffected by the geophysical indirect effect, analysis of the gravity field and the geoid can hardly justify the present lithospheric models and the more interesting topic of changes within the lithospheric subduction direction. However, the analysis shows that the lithosphere geometry of Lippitsch et al. (2003) can be easily combined with a crustal model and adjusted to the observed anomalies.

It has to be mentioned that the results of studies by Kummerow et al. (2004) and Panza et al. (2003) point to different lithospheric geometries. Due to the small density contrast at the lithosphere–asthenosphere boundary and the uncertainties on its value as shown above, a comparative analysis of the different proposed models is beyond the limitations of a potential field study. Another factor that would strongly influence our results is the presence of sub-lithospheric density anomalies. These may generate general trends, visible in the geoid undulations. Recent tomographic studies show that such asthenospheric events exist below the Alpine area (e.g. Becker and Boschi, 2002).

The complexity of the collision of the Adriatic and European plate leads to the superposition of a variety of density inhomogeneities at different depth levels, which are difficult to distinguish. A better control on the crustal structure and associated velocities will increase the chances to detect changes in the lithospheric density structure.

Changes in the lithospheric subduction direction as suggested by the tomographic study of Lippitsch et al. (2003) would be difficult to identify in the case of two colliding continental plates. A good example where the subduction of a lithospheric plate leads to a prominent geoid and gravity anomaly is in the Andes. Here an oceanic plate (Nazca plate) subducts below a continental plate (South American plate) and the different compositions of the continental and oceanic plates require different densities. When the gravity effect of the downgoing Nazca Plate is removed from both Bouguer and isostatic residual anomalies (Airy and Vening–Meinesz type), the remaining field can be correlated with mean topographic heights to identify areas of disturbed isostatic equilibrium. Then it can be observed that most of the morphological Andean units are close to isostatic equilibrium; in particular Airy type equilibrium can be found in the Main Cordillera (Götze and Kirchner, 1997; Götze and Krause, 2002).

As the Alps are affected by continent–continent collisions, the compositional differences between the plates are only minor, and the crustal domains have overprinted the influence of the deep lithospheric geometries and densities on the gravity field as well as the geoid undulations. However, the inferred isostatic lithosphere thickness shows a division of the lithospheric root similar to the tomographic results. To strengthen the arguments for a change in subduction direction and to test further the lithospheric geometry, more sophisticated methods as dynamic modelling should be carried out. The necessary simplification of the input models is another problem, which might cover the structure of the Eastern Alpine lithosphere.

Acknowledgements

The authors express their gratitude to Jörg Ansorge, Edi Kissling, Jörn Kummerow, Ewald Lueschen and the members of the TRANSALP Working Group for providing new results from the seismic and tomographic investigations. We thank Tim Redfield for improving the English grammar and syntax and Gabriel Strykowski and Bruno Meurers for carefully reviewing the manuscript. Gravity data for Austria, Italy and Germany were kindly provided by the University of Vienna, the Bureau Gravimetrique International (Toulouse), ENI/AGIP Italia (Milano), BBT (Innsbruck) and GGA (Hannover). The density modelling was done using the IGMAS software (http://www.gravity.uni-kiel.de/igmas/). The study was supported by the Deutsche Forschungsgemeinschaft (Go 380/19-1, 19-3, 19-4), the Italian Ministry funding COFIN, the German–Italian research program VIGONI and NGU network founding.

References

Banks, R.J., Francis, S.C., Hipkin, R.G., 2001. Effects of loads in the upper crust on estimates of the elastic thickness of the lithosphere. Geophysical Journal International 145, 291–299.

Babuška, V., Plomerová, J., Granet, M., 1990. The deep lithosphere in the Alps: a model inferred from P residuals. Tectonophysics 176, 137–165.

Becker, T.W., Boschi, L., 2002. A comparison of tomographic and geodynamic mantle models. Geochemical, Geophysical, Geosystem 3. doi:10.1029/2001GC000168.

Berthelsen, A., Burrolet, P., Dal Piaz, G.V., Franke, W., Trümpy, R., 1992. Tectonics. In: Blundell, D., Freeman, R., Mueller, St. (Eds.), A Continent Revealed: The European Geotraverse. Cambridge University Press.

Braitenberg, C., Pettenati, F., Zadro, M., 1997. Spectral and classical methods in the evaluation of Moho undulations from gravity data: the NE-Italian Alps and isostasy. Journal of Geodynamics 23, 5–22.

Braitenberg, C., Ebbing, J., Götze, H.-J., 2002. Inverse modelling of elastic thickness by convolution method — the Eastern Alps as a case example. Earth and Planetary Science Letters 202, 387–404.

Cassinis, R., Federici, F., Galmozzi, A., Scarascia, S., 1997. A 3D gravity model of crustal structure in the Central-Eastern Alpine sector. Annali di Geofisica XL (5), 1095–1107.

Dziewonski, A.M., Anderson, D.L., 1981. Preliminary reference earth model. Physics of the Earth and Planetary Interiors 25, 297–356.

Ebbing, J., 2004. The crustal structure of the Eastern Alps from a combination of 3D gravity modelling and isostatic investigations. Tectonophysics 380 (1–2), 80–104.

Ebbing, J., Braitenberg, C., Götze, H.J., 2001. Forward and inverse modelling of gravity revealing insight into crustal structures of the Eastern Alps. Tectonophysics 337 (3–4), 191–208.

Giese, P., Buness, H., 1992. Moho depth. In: Blundell, D., Freeman, R., Mueller, St. (Eds.), A Continent Revealed: The European Geotraverse. Cambridge University Press.

Götze, H.-J., Kirchner, A., 1997. Interpretation of gravity and geoid in the Central Andes between 20° and 29° S. Journal of South American Earth Sciences 10 (2), 179–188.

Götze, H.-J., Krause, S., 2002. The Central Andean gravity high, a relic of an old subduction complex? Journal of South American Earth Sciences 14 (8), 799–811.

Götze, H.-J., Meurers, B., Schmidt, S., Steinhauser, P., 1991. On the isostatic state of the Eastern Alps and the Central Andes — a statistical comparison. In: Harmon, R.S., Rapela, C.W. (Eds.), Andean Magmatism and its Tectonic Setting, GSA Special Volume, pp. 279–290.

Hackney, R.I., Featherstone, 2003. Geodetic versus geophysical perspectives of the gravity anomaly. Geophysical Journal International 154 (1), 35–43.

Klingele, E., Kissling, E., 1982. Schwere-Anomalien und isostatische Modelle in der Schweiz. Geodätisch-Geophysikalische Arbeiten in der Schweiz, Bd., vol. 35. Schweizerische Geodätische Kommission.

Kissling, E., 1993. Deep structures of the Alps — what do we really know? Physics of the Earth and Planetary Interiors 79, 87–112.

Kummerow, J., 2002. Strukturuntersuchungen in den Ostalpen anhand des teleseismischen TRANSALP-Datensatzes. PhD thesis at Freie Universität Berlin.

Kummerow, J., Kind, R., Oncken, O., Giese, P., Ryberg, T., Wylegalla, K., TRANSALP Working Group, 2004. A natural and controlled source seismic profile through the Eastern Alps: TRANSALP. Earth and Planetary Science Letters 225, 115–129.

Lelgemann, D., Kuckuck, H., 1992. Geoid undulations and horizontal gravity disturbance components. In: Blundell, D., Freeman, R., Mueller, St. (Eds.), A Continent Revealed: the European Geotraverse. Cambridge University Press.

Lillie, R.J., Bielik, M., Babuška, V., Plomerová, J., 1994. Gravity modelling of the lithosphere in the Eastern Alpine–Western Carpathian–Pannonian Basin region. Tectonophysics 231, 215–235.

Lippitsch, R., 2002. Lithosphere and upper mantle P-wave velocity structure beneath the Alps by high-resolution teleseismic tomography. PhD thesis, ETH Zürich.

Lippitsch, R., Kissling, E., Ansorge, J., 2003. Upper mantle structure beneath the Alpine orogen from high-resolution teleseismic tomography. Journal of Geophysical Research 108, 2376. doi:10.1029/2002JB002016.

Panza, G.F., Raykova, R., Chimera, G., Aoudia, A., 2003. Multiscale surface wave tomography in the Alps. TRANSALP Conference-Memorie di Scienze Geologiche 54, 55–56.

Ranalli, G., 1995. Rheology of the Earth. Chapman and Hall, London, p. 413.

Scarascia, S., Cassinis, R., 1997. Crustal structures in the central-eastern Alpine sector: a revision of the available DSS data. Tectonophysics 271, 157–188.

Sobolev, S., Babeyko, A., 1994. Modeling of mineralogical composition, density and elastic wave velocities in anhydrous magmatic rocks. Surveys in Geophysics 15, 515–544.

Suhadolc, P., Panza, G.F., Mueller, S., 1990. Physical properties of the lithosphere — asthenosphere system in Europe. Tectonophysics 176, 123–135.

TRANSALP Working Group, 2001. European orogenic processes research transects the Eastern Alps. EOS, 82 (40). p.453 and 460–461.

TRANSALP Working Group, 2002. First deep seismic reflection images of the Eastern Alps reveal giant crustal wedges and transcrustal ramps. Geophysical Research Letters 29. doi:10.1029/2002GL014911.

U.S. Geological Survey, 2000. GTOPO30 — Global topographic data. http://edcdaac.usgs.gov/gtopo30/gtopo30.html.

Wagini, A., Steinhauser, P., Meurers, B., 1988. Isostatic residual gravity map of Austria. U.S. Geological Survey Open File Report 87–402.

Zanolla, C., Braitenberg, C., Ebbing, J., Bernabini, M., Bram, K., Gabriel, G., Götze, H.-J., Giammetti, S., Meurers, B., Nicolich, R., Palmieri, F., 2006. New gravity maps of the Eastern Alps and significance for the crustal structures. Tectonophysics 414, 127–143. (this volume).